

Microwave Synthesis, Crystal Structure and Magnetic Behavior of a Schiff Base Trinuclear Nickel Cluster

Shu-Hua Zhang,^{*[a]} Ming-Feng Tang,^[b] and Cheng-Min Ge^[a]

Keywords: Cluster compounds; Magnetic properties; Microwave chemistry; Nickel; N,O ligands

Abstract. The reaction of $\text{Ni}(\text{ClO}_4)_2 \cdot 6\text{H}_2\text{O}$ with 2-hydroxybenzaldehyde and an aqueous solution of methylamine in acetonitrile/MeOH under microwave irradiation and controlled temperature/pressure leads to formation of trinuclear cluster $[\text{Ni}_3(\text{mimp})_5(\text{CH}_3\text{CN})]\text{ClO}_4$ (**1**; mimp = 2-methyliminomethylphenolate anion)

in only 29 min and also results in higher yields in contrast to other synthesis methods. Complex **1** displays dominant ferromagnetic interactions through $\mu_3\text{-O}$ (oxidophenyl) and $\mu_2\text{-O}$ (oxidophenyl) binding modes.

Introduction

In the past decade, much attention has been given to the design and synthesis of polynuclear clusters since the discovery of single-molecule magnets (SMMs) [1–5]. The search for key ligands is important for advancing these investigations. Recently, the evergreen Schiff base ligands have been widely used in the synthesis of magnetic molecular clusters [6–9]. Previous research showed that metal complexes constructed by derivatives of the sap^{2-} ligand (sap^{2-} = 2-salicylideneamino-1-propanolate anion) are usually polynuclear clusters with favored ferromagnetic coupling through $\mu_3\text{-O}$ bridges and tend to be characterized by SMM behavior. Here we chose the analogous ligand mimp (mimp = 2-methyliminomethylphenolate anion) to serve as a chelating/bridging ligand to bring metal ions into new type of polynuclear cluster. The vast majority of paramagnetic cluster compounds were produced by “conventional” techniques involving mixed metal ions and ligands at a temperature limited by the boiling point of a common solvent at atmospheric pressure. New preparative routes for the synthesis of molecular clusters under nonambient conditions have been developed. Recently, higher-temperature solvothermal methods to synthesize clusters were explored [1–5, 10]. More recently, microwave heating, as a new and

extremely attractive method for synthesizing polynuclear clusters, has also been introduced into solvothermal methods. It provides a clean, cheap, and convenient method of heating that can result not only in higher yields and shorter reaction times but also in the formation of completely new products [11–16]. Indeed, here we demonstrate the microwave-assisted synthesis of a trinuclear complex that cannot be synthesized under ambient or solvothermal conditions.

Results and Discussion

Crystal Structure of $[\text{Ni}_3(\text{mimp})_5(\text{CH}_3\text{CN})]\text{ClO}_4$ (**1**)

Complex **1** crystallizes in the monoclinic space group $P2_1/n$ (Figure 1). The core of the molecule contains three Ni^{II} ions arranged in an equilateral triangle bridged by two central $\mu_3\text{-O}$ [oxidophenyl; Ni1-O1-Ni2 87.13(5), Ni1-O1-Ni3 83.79(5), Ni2-O1-Ni3 88.73(5), Ni1-O4-Ni2 87.16(6), Ni1-O4-Ni3 87.53(6), Ni2-O4-Ni3 88.09(6)°] with an $\text{Ni}\cdots\text{Ni}$ distance of 2.9 Å, which is shorter than that of $[\text{Ni}_3(\text{N}_3)_3(\text{O}_2\text{CMe})_3(\text{py})_5]$ (py = pyridine) [12]. Three nickel ions are further connected via three $\mu_2\text{-O}$ [oxidophenyl; O2, O3, O5 ; Ni2-O2-Ni3 86.32(5), Ni1-O3-Ni2 86.31(6), Ni1-O5-Ni3 86.66(5)°]. The coordination of the three nickel ions is completed by five nitrogen atoms of five mimp ligands and one terminal acetonitrile molecule. All three nickel ions are six-coordinate and adopt distorted octahedral geometries with *cis* and *trans* angles in the ranges 72.6–105.0° and 150.6–169.1°, respectively, but the coordination environment of the Ni1 ion is different from those of Ni2 and Ni3. The Ni2 and Ni3 atoms are coordinated by four oxygen atoms and two nitrogen atoms from four different mimp ligands, while Ni1 is coordinated by four oxygen atoms and one nitrogen atom from four different mimp ligands and one nitrogen atom from the terminal acetonitrile molecule. All three nickel ions are in the 2+ oxidation state, as evidenced by bond

* Prof. Dr. S.-H. Zhang
Fax: +86-773-5896-671
E-Mail: zsh720108@163.com

[a] Key Laboratory of Nonferrous Metal Materials and Processing Technology
Department of Material and Chemical Engineering
Guilin University of Technology, Ministry of Education
Guilin, 541004, P. R. China

[b] Department of Foreign Languages
Guilin University of Technology
Guilin, 541004, P. R. China

Supporting information for this article is available on the WWW under www.zaac.wiley-vch.de or from the author.

valence sum calculations, charge-balance considerations, and the presence of typical bond lengths for Ni^{II} . Recently, it was shown that intermolecular $\text{C}-\text{H}\cdots\text{Cl}-\text{M}$ hydrogen bonds provide a pathway for intermolecular magnetic exchange interaction [17]. This type of hydrogen bonds is not been observed in **1**. On the other hand, there are no significant intercluster interactions except for very weak $\text{C}-\text{H}\cdots\text{O}$ hydrogen bonds ($\text{C}36\cdots\text{O}6^{\text{i}}$ 3.410(4) Å, $\text{C}42\cdots\text{O}6^{\text{ii}}$ 3.194(4) Å, symmetry code: i) $x, y, 1 + z$; ii) $3/2 - x, 1/2 + y, 3/2 - z$; see Figure S1, Supporting Information). The intermolecular magnetic exchange interactions would be anticipated to be the weakest among them. Therefore, intermolecular magnetic exchange interactions propagated by this pathway may be negligible.

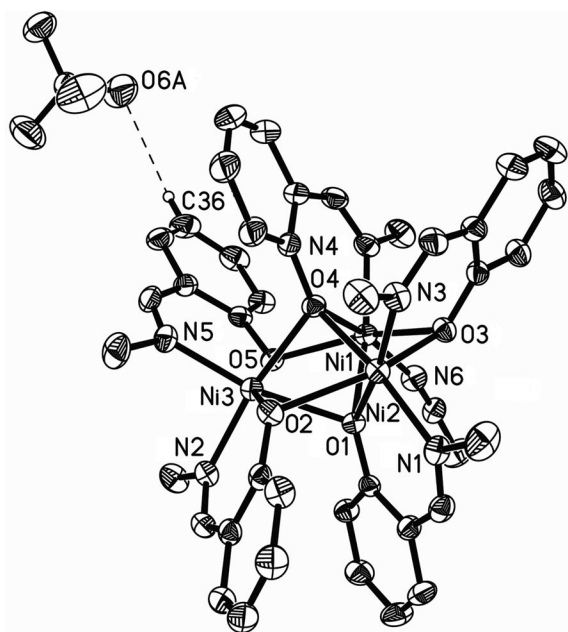
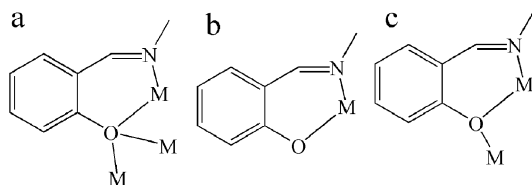


Figure 1. Structure of **1**. Some of the hydrogen atoms were omitted.

To the best of our knowledge, two coordination modes of the 2-methyliminomethylphenolate ligand have been reported (Scheme 1b and c) [18–23]; its unusual tetradentate $\mu_3:\eta^1:\eta^3$ coordination mode in **1** (Scheme 1a) has not appeared before.



Scheme 1. Coordination modes of the 2-methyliminomethylphenolate ligand.

Magnetic Properties

The magnetic susceptibility of **1** was measured on a crushed single-crystalline sample. The dc susceptibility of **1** was measured under an applied field of 1 kOe at 2 to 300 K.

For **1**, at room temperature, spin–orbital coupling of Ni^{II} ions gives rise to a $\chi_{\text{M}}T$ product of $4.56 \text{ cm}^3 \text{ K mol}^{-1}$, which is much higher than the spin-only value of $3.0 \text{ cm}^3 \text{ K mol}^{-1}$ for three noninteracting high-spin Ni^{II} ions assuming $g = 2.0$. The $\chi_{\text{M}}T$ value of **1** at a temperature of 300 K lies in the range of other trinuclear nickel clusters, which have $\chi_{\text{M}}T$ values from 2.75 to $5.31 \text{ cm}^3 \text{ K mol}^{-1}$ [12, 24–28]. With decreasing T , $\chi_{\text{M}}T$ of **1** smoothly increases to $8.11 \text{ cm}^3 \text{ K mol}^{-1}$ at ca. 2.8 K, and then smoothly falls to $8.02 \text{ cm}^3 \text{ K mol}^{-1}$ at 2 K (Figure 2). Similar magnetic behavior was observed for $[\text{Ni}_3(\text{N}_3)_3(\text{O}_2\text{CMe})_3(\text{py})_5]$ [12].

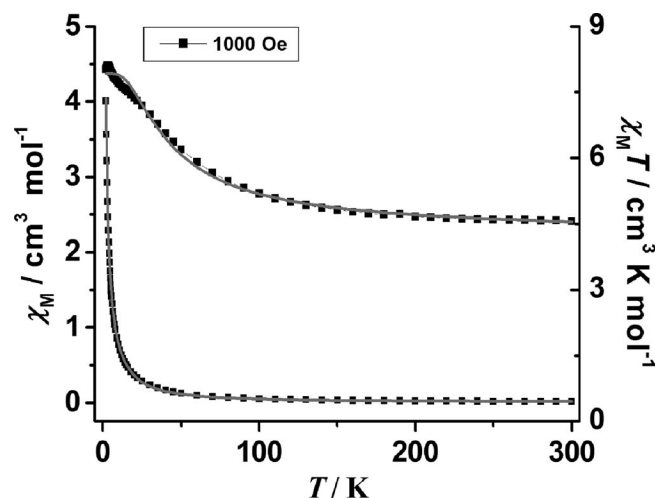


Figure 2. Plot of χ_{M} and $\chi_{\text{M}}T$ versus T for complex **1**, the solid lines correspond to the best theoretical fits.

The temperature dependence of the reciprocal susceptibility χ_{M}^{-1} above 50 K follows the Curie–Weiss law [$\chi_{\text{M}} = C/(T - \theta)$] with a Weiss constant of $\theta = 5.63 \text{ K}$ and Curie constant of $C = 4.55 \text{ cm}^3 \text{ K mol}^{-1}$ (Figure S2, Supporting Information). The larger positive Weiss constant indicates dominant intramolecular ferromagnetic interaction between adjacent Ni^{II} ions through the two kinds of oxygen exchange bridges (Figure 1). The low-temperature maximum is indicative of an $S = 3$ ground state (with $g = 2.30$). This pattern is compatible with moderate ferromagnetic coupling [29–31]. The sudden decrease in $\chi_{\text{M}}T$ at low temperature is assigned to zero-field splitting in the ground state, Zeeman effects, or intermolecular antiferromagnetic interactions.

Further evidence of ferromagnetic coupling between Ni^{II} ions can be observed in variable-field magnetization curves (Figure S3, Supporting Information). At low fields from 0 to 1 T the magnetization of complex **1** sharply increases. Above 1 T the magnetization slowly increases and saturates at $6.40 N\mu_{\text{B}}$ at 5 T.

Alternating-current susceptibility measurements on **1** were carried out in the range 2–10 K at 50 and 499 Hz (Figure 3). The absence of out-of-phase ac signals above 2 K indicates that **1** does not behave as an SMM. A possible

explanation for this behavior of **1** could come from the intermolecular magnetic interactions propagated by this pathway, which may be negligible.

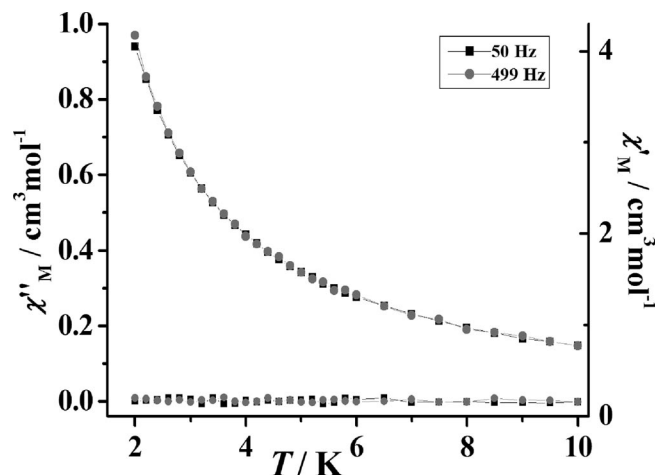


Figure 3. In-phase and out-of-phase ac susceptibility of **1**.

Examination of the bond lengths and angles between the Ni^{II} centers in **1** for magnetostructural correlations revealed an obvious trend based on structural parameters. When the values reported for the different Ni^{II} clusters are compared, some general observations can be made. Three intracuster Ni^{II}–Ni interactions are nearly equilateral with the exchange angles in the range from 83.79 to 87.73°, and tend to yield orthogonality for Ni^{II}–Ni ferromagnetic superexchange pathways [32, 33]. Employing the isotropic spin Hamiltonian in Equation (1) and χ_M in Equation (2), allowed us to satisfactorily model the data with the parameters $J = +5.18 \text{ cm}^{-1}$ and $g = 2.30$ (Figure 2).

$$\hat{H} = -2J(\hat{S}_1\hat{S}_2 + \hat{S}_2\hat{S}_3 + \hat{S}_3\hat{S}_1) \quad (1)$$

$$\chi_M = \frac{2Ng^2\beta^2}{kT} \times \frac{3e^{2J/kT} + 10e^{6J/kT} + 14e^{12J/kT}}{1 + 9e^{2J/kT} + 10e^{6J/kT} + 7e^{12J/kT}} \quad (2)$$

Conclusions

In summary, we have synthesized a triangular nickel cluster with the composition $[\text{Ni}_3(\text{mimp})_5(\text{CH}_3\text{CN})]\text{ClO}_4$ (**1**) where mimp the deprotonated form of 2-methylimino-methylphenol, which prevents effective intermolecular interaction. Magnetic measurements show that **1** displays dominant ferromagnetic interactions.

Experimental Section

General: All reagents were commercially available and used without further purification. Microwave synthesis was performed with a WX-4000 microwave digestion system. Elemental analyses for C, H, N were performed on an Elemental Vario-EL CHNS elemental analyzer. IR spectra were recorded on Bio-Rad FTS-7 spectro-

photometer in the 4000–400 cm^{-1} region by using KBr pellets. Variable-temperature magnetic susceptibility measurements were carried out with a SQUID MPMS XL7 magnetometer in the temperature range 2–300 K in a magnetic field of 1000 Oe. The molar magnetic susceptibility was corrected for the sample holder and diamagnetic contributions of all constituent atoms by using Pascal's constants. The crystal structure was determined by single-crystal X-ray diffraction, and SHELXS-97 and SHELXL-97 software was used for structure solution and refinement correspondingly.

Preparation of $[\text{Ni}_3(\text{mimp})_5(\text{CH}_3\text{CN})]\text{ClO}_4$ (1**):** 2-Hydroxybenzaldehyde (0.244 g, 2 mmol), aqueous methylamine solution (0.5 mL, 25 %), triethylamine (0.6 mL), $\text{Ni}(\text{ClO}_4)_2 \cdot 6\text{H}_2\text{O}$ (0.361 g, 1 mmol), methanol (15 mL), and acetonitrile (15 mL) were placed in a 60 mL Teflon-lined autoclave, which was then inserted into the cavity of a microwave reactor. The reaction mixture was maintained at $T = 120^\circ\text{C}$, power = 300 W, and $p = 7.2 \text{ atm}$ for a total of 29 min, followed by cooling (ca. 120 min). The resulting solution was then filtered. Green blocklike crystals suitable for X-ray structure analysis were grown at room temperature by slow evaporation for 6 d. The crystals were collected by filtration, washed with methanol and dried in air. Phase-pure crystals of **1** were obtained by manual separation. Yield: 87 % (based on Ni). $\text{C}_{42}\text{H}_{43}\text{N}_6\text{ClO}_9\text{Ni}_3$: C, 51.09; H, 4.39; N, 8.51 %. Found: C, 51.02; H, 4.45; N, 8.47 %. Major IR absorptions: 1638 $\nu_s(\text{C}=\text{N})$ [34], 1038, 950 $\text{cm}^{-1} \nu(\text{ClO}_4^-)$.

Preparation of $\text{Ni}(\text{mimp})_2$ [35]: A solution of 2-hydroxybenzaldehyde (0.244 g, 2 mmol), aqueous methylamine solution (0.5 mL, 25 %), and triethylamine (0.6 mL) in methanol (15 mL) was added slowly to a solution of $\text{Ni}(\text{ClO}_4)_2 \cdot 6\text{H}_2\text{O}$ (0.361 g, 1 mmol) in acetonitrile (15 mL). The mixture was stirred and heated to reflux for 2 h at 353 K. The solution was filtered and the filtrate left to stand at room temperature. Red sheet crystals suitable for X-ray diffraction were obtained in 54 % yield (based on Ni). $\text{C}_{16}\text{H}_{16}\text{N}_2\text{O}_2\text{Ni}$: C, 58.77; H, 4.93; N, 8.56 %. Found: C, 58.71; H, 5.05; N, 8.52 %. The unit cell parameters of the red sheet crystals are the same as in reference [35].

X-ray crystallography: A green block crystal of complex **1** having approximate dimensions $0.318 \times 0.282 \times 0.262 \text{ mm}$ was selected and mounted on a glass fiber. All measurements were made on a Bruker Smart 1000 CCD diffractometer with graphite-monochromated Mo- K_α radiation ($\lambda = 0.71073 \text{ \AA}$). A total of 7615 reflections were collected by a ω – ϕ scan technique at 293(2) K in the range of $2.41 \leq \theta \leq 25.10^\circ$ with index ranges of $-20 \leq h \leq 20$, $-14 \leq k \leq 14$, $-24 \leq l \leq 24$, of which 6294 were independent ($R_{\text{int}} = 0.0251$). Empirical absorption corrections by SADABS were carried out. The structure was solved by direct methods with the SHELXS-97 program [36] and refined with SHELXL-97 [37] by full-matrix least-squares techniques on F^2 . All non-hydrogen atoms were refined anisotropically, while all hydrogen atoms were added in calculated positions, included in the stage of refinement with isotropic thermal parameters $U(\text{H}) = 1.2U_{\text{eq}}(\text{C})$ [$U(\text{H}) = 1.5U_{\text{eq}}(\text{CMe})$]. Final $R = 0.0274$ and $wR = 0.0753$ ($R = \Sigma||F_o| - |F_c||/\Sigma|F_o|$, $wR_2 = [\Sigma w(F_o^2 - F_c^2)^2/\Sigma w(F_o^2)^2]^{1/2}$, $w = 1/[\sigma^2(F_o^2) + 0.0397P + 1.0351P]$, where $P = (F_o^2 + 2F_c^2)/3$). A summary of crystallographic data is given in Table 1. Selected bond lengths and angles are listed in Table 2. Atomic coordinates are contained in Table S2 (Supporting Information). CCDC-713023 contains the supplementary crystallographic data for this paper. These data can be obtained free of charge from The Cambridge Crystallographic Data Centre via www.ccdc.cam.ac.uk/data_request/cif.

Table 1. Crystal data and structure refinement for **1**.

Formula	C ₄₂ H ₄₃ Ni ₃ O ₉ N ₆ Cl
Formula weight/g mol ⁻¹	987.34
Crystal system	monoclinic
Space group	<i>P</i> 2 ₁ / <i>n</i> (No. 14)
<i>a</i> /Å	17.1676(16)
<i>b</i> /Å	12.2894(12)
<i>c</i> /Å	20.855(2)
β /°	103.1380(10)
<i>V</i> /Å ³	4284.8(7)
<i>Z</i>	4
ρ_{calcd} /g cm ⁻³	1.531
μ /mm ⁻¹	1.429
<i>F</i> (000)	2040
Crystal size/mm	0.318 × 0.282 × 0.262
θ range/°	2.41 ≤ θ ≤ 25.10
No. of measured reflns	31119
No. of unique reflns	7615
No. of observed [<i>I</i> > 2 σ (<i>I</i>)] reflns	6294
Goodness-of-fit on <i>F</i> ²	1.066
Final <i>R</i> indices [<i>I</i> > 2 σ (<i>I</i>)]	<i>R</i> ₁ = 0.0274, <i>wR</i> ₂ = 0.0700
<i>R</i> indices (all data)	<i>R</i> ₁ = 0.0375, <i>wR</i> ₂ = 0.0753
Factors of weighting scheme*	0.0397, 1.0351
Residual electron density/e Å ⁻³	0.412, -0.310

* Standard SHELXL weighting scheme $w = 1/[\sigma^2(F_o^2) + (aP)^2 + bP]$ where $P = (F_o^2 + 2F_c^2)/3$

Table 2. Selected bond lengths/Å and angles/° for **1**.

Ni1–N4	2.021(2)	Ni1–O4	2.0235(15)
Ni1–N6	2.032(2)	Ni1–O1	2.1123(14)
Ni1–O3	2.1288(15)	Ni1–O5	2.1358(215)
Ni2–N3	2.010(2)	Ni2–N1	2.016(2)
Ni2–O1	2.0354(14)	Ni2–O3	2.0502(15)
Ni2–O4	2.1224(15)	Ni2–O2	2.2690(15)
Ni3–N2	1.9862(19)	Ni3–N5	2.0124(19)
Ni3–O2	2.0332(15)	Ni3–O5	2.0388(15)
Ni3–O4	2.1179(15)	Ni3–O1	2.1780(14)
O4–Ni1–N6	169.05(7)	N4–Ni1–O1	167.89(7)
O4–Ni1–O1	75.86(6)	N6–Ni1–O1	93.19(7)
N4–Ni1–O4	92.03(7)	N4–Ni1–N6	98.92(8)
N4–Ni1–O3	101.27(7)	O4–Ni1–O3	79.72(6)
N6–Ni1–O3	98.11(7)	O1–Ni1–O3	76.88(6)
N4–Ni1–O5	97.61(7)	O4–Ni1–O5	80.28(6)
N6–Ni1–O5	98.03(7)	O1–Ni1–O5	80.56(5)
O3–Ni1–O5	152.85(6)	N3–Ni2–N1	99.92(8)
N3–Ni2–O1	167.29(7)	N1–Ni2–O1	92.02(7)
N3–Ni2–O3	93.28(7)	N1–Ni2–O3	99.35(7)
O1–Ni2–O3	80.39(6)	N3–Ni2–O4	92.67(7)
N1–Ni2–O4	167.40(7)	O1–Ni2–O4	75.39(6)
O3–Ni2–O4	79.28(6)	N3–Ni2–O2	105.07(7)
N1–Ni2–O2	99.84(7)	O1–Ni2–O2	76.88(6)
O3–Ni2–O2	150.60(6)	O4–Ni2–O2	77.13(6)
N2–Ni3–O2	94.45(7)	N2–Ni3–N5	92.35(8)
N5–Ni3–O2	104.24(7)	N2–Ni3–O5	100.15(7)
N5–Ni3–O5	92.86(7)	O2–Ni3–O5	157.02(6)
N2–Ni3–O4	171.38(7)	N5–Ni3–O4	96.22(7)
O2–Ni3–O4	82.59(6)	O5–Ni3–O4	80.37(6)
N2–Ni3–O1	98.94(7)	N5–Ni3–O1	168.00(7)
O2–Ni3–O1	79.05(6)	O5–Ni3–O1	81.22(6)
O4–Ni3–O1	72.58(5)		

Supporting Information (see footnote on the first page of this article): Packing diagram for **1** (Figure S1), plot of χ_M^{-1} vs. *T* for **1** (Figure S2), field dependence of magnetization for **1** at 2 K (Figure S3), $\chi_M T$ values at room temperature for different trinuclear nickel

clusters (Table S1), and atomic coordinates ($\times 10^4$) and equivalent isotropic displacement parameters ($\text{\AA}^2 \times 10^3$) for **1** (Table S2).

Acknowledgement

This project was supported by Guangxi Key Laboratory for Advance Materials and New Preparation Technology (No: 0842003-25) and the Young Science Foundation of Guangxi Province of China (No: 0832085).

References

- [1] *From the Molecular to the Nanoscale: Synthesis, Structure, and Properties*, Vol. 7 (Eds.: M. Fujita, A. Powell, C. Creutz), Elsevier-Ltd., Oxford, **2004**.
- [2] D. Gatteschi, R. Sessoli, *Angew. Chem. Int. Ed.* **2003**, *42*, 268.
- [3] D. Yoshihara, S. Karasawa, N. Koga, *J. Am. Chem. Soc.* **2008**, *130*, 10460.
- [4] C. C. Beedle, C. J. Stephenson, K. J. Heroux, W. Wernsdorfer, D. N. Hendrickson, *Inorg. Chem.* **2008**, *47*, 10798.
- [5] K. W. Galloway, A. M. Whyte, W. Wernsdorfer, J. Sanchez-Benitez, K. V. Kamenev, A. Parkin, R. D. Peacock, M. Murrie, *Inorg. Chem.* **2008**, *47*, 7438.
- [6] C. J. Milios, A. Prescimone, A. Mishra, S. Parsons, W. Wernsdorfer, G. Christou, S. P. Perlepes, E. K. Brechin, *Chem. Commun.* **2007**, 153.
- [7] T. C. Stamatatos, D. Foguet-Albiol, S.-C. Lee, C. C. Stoumpos, C. P. Raptopoulou, A. Terzis, W. Wernsdorfer, S. O. Hill, S. P. Perlepes, G. Christou, *J. Am. Chem. Soc.* **2007**, *129*, 9484.
- [8] C. J. Milios, R. Inglis, A. Vinslava, R. Bagai, W. Wernsdorfer, S. Parsons, S. P. Perlepes, G. Christou, E. K. Brechin, *J. Am. Chem. Soc.* **2007**, *129*, 12505.
- [9] D. Z. Gao, Y. Q. Sun, D. Z. Liao, Z. H. Jiang, S. P. Yan, Z. *Anorg. Allg. Chem.* **2008**, *634*, 1950.
- [10] R. H. Laye, E. J. L. McInnes, *Eur. J. Inorg. Chem.* **2004**, 2811.
- [11] C. J. Milios, A. G. Whittaker, E. K. Brechin, *Polyhedron* **2007**, *26*, 1927 and references therein.
- [12] J. Milios, A. Prescimone, J. Sanchez-Benitez, S. Parsons, M. Murrie, E. K. Brechin, *Inorg. Chem.* **2006**, *45*, 7053.
- [13] C. J. Milios, A. Vinslava, A. G. Whittaker, S. Parsons, W. Wernsdorfer, G. Christou, S. P. Perlepes, E. K. Brechin, *Inorg. Chem.* **2006**, *45*, 5272.
- [14] I. A. Gass, C. J. Milios, A. G. Whittaker, F. P. A. Fabiani, S. Parsons, M. Murrie, S. P. Perlepes, E. K. Brechin, *Inorg. Chem.* **2006**, *45*, 5281.
- [15] C. P. Raptopoulou, A. K. Boudalis, Y. Sanakis, V. Psycharis, J. M. Clemente-Juan, M. Fardis, G. Diamantopoulos, G. Papavassiliou, *Inorg. Chem.* **2006**, *45*, 2317.
- [16] S. H. Zhang, Y. Song, H. Liang, M. H. Zeng, *Cryst. Eng. Commun.* **2009**, *11*, 865–872.
- [17] W. Wernsdorfer, N. Aliaga-Alcalde, D. N. Hendrickson, G. Christou, *Nature* **2002**, *416*, 406.
- [18] X. Y. Li, L. Y. Huang, H. J. Sun, M. Li, Z. *Anorg. Allg. Chem.* **2005**, *631*, 3096.
- [19] H. Torayama, H. Asada, M. Fujiwara, T. Matsushita, *Polyhedron* **1998**, *17*, 3859.
- [20] F. Corazza, E. Solari, C. Floriani, A. Chiesi-Villa, C. Guastini, *J. Chem. Soc., Dalton Trans.* **1990**, 1335.
- [21] C. R. Cornman, K. M. Geiser-Bush, S. P. Rowley, P. D. Boyle, *Inorg. Chem.* **1997**, *36*, 6401.
- [22] E. Sinn, W. T. Robinson, *J. Chem. Soc., Chem. Commun.* **1972**, 359.
- [23] H. Shimanouchi, Y. Sasada, H. Yokoi, *Acta Crystallogr. Sect. B* **1979**, *35*, 162.
- [24] S. Yamada, M. Yasui, T. Nogami, T. Ishid, *Dalton Trans.* **2006**, 1622.

- [25] T. Beissel, F. Birkelbach, E. Bill, T. Glaser, F. Kesting, C. Krebs, T. Weyhermüller, K. Wieghardt, C. Butzlaff, A. X. Trautwein, *J. Am. Chem. Soc.* **1996**, *118*, 12376.
- [26] K. O. Kongshaug, H. Fjellvang, *Solid State Sci.* **2003**, *5*, 303–310.
- [27] Z. Tomkowicz, S. Ostrovsky, H. Müller-Bunz, A. J. Hussein Eltmimi, M. Rams, D. A. Brown, W. Haase, *Inorg. Chem.* **2008**, *47*, 6956.
- [28] A. Escuer, I. Castro, F. Mautner, M. S. E. Fallah, R. Vicente, *Inorg. Chem.* **1997**, *36*, 4633.
- [29] B. Cage, F. A. Cotton, N. S. Dalal, E. A. Hillard, B. Rakvin, C. M. Ramsey, *J. Am. Chem. Soc.* **2003**, *125*, 5270.
- [30] P. L. Feng, C. C. Beedle, W. Wernsdorfer, C. Koo, M. Nakano, S. Hill, D. N. Hendrickson, *Inorg. Chem.* **2007**, *46*, 8126.
- [31] M.-L. Tong, M. Monfort, J. M. C. Juan, X.-M. Chen, X.-H. Bu, M. Ohba, S. Kitagawa, *Chem. Commun.* **2005**, 233.
- [32] J. J. Borrás-Almenar, J. M. Clemente-Juan, E. Coronado, B. Tsukerblat, *Inorg. Chem.* **1999**, *38*, 6081.
- [33] J. J. Borrás-Almenar, J. M. Clemente-Juan, E. Coronado, B. Tsukerblat, *J. Comput. Chem.* **2001**, *22*, 985.
- [34] S. H. Zhang, Y. M. Jiang, Z. Liu, K. B. Yu, *Acta Crystallogr. Sect. E* **2005**, *61*, m446.
- [35] B. Kamenar, B. Kaitner, G. Ferguson, T. N. Waters, *Acta Crystallogr. Sect. C* **1990**, *46*, 1920.
- [36] G. M. Sheldrick, *SHELXS-97*: Program for the Solution of Crystal Structures, University of Göttingen, Germany **1997**.
- [37] G. M. Sheldrick, *SHELXL-97*: Program for the Refinement of Crystal Structures, University of Göttingen, Germany **1997**.

Received: January 16, 2009
Published Online: May 11, 2009